Journal of Structural Geology, Vol. 15, No. 7, pp. 831 to 847, 1993
Printed in Great Britain

0191-8141/93 $06.00+0.00

Structural aspects of diapiric mélange emplacement: the Duck Creek Diapir

KEVIN M. BROWN* and DANIEL L. ORANGE

Earth Science Board, University of California, Santa Cruz, CA 95064, U.S.A.

(*Received* 23 *January* 1991; *accepted in revised form* 31 *August* 1992)

Abstract—The Duck Creek mélange is one of a series of diapiric mud intrusions into the slope cover sequence of the Cascadia Accretionary Wedge. The diapir originated deep within the accreted Hoh sequences and has intruded approximately 1 km up into the 2–3 km thick Pliocene Quinault slope cover sequences at its current level of exposure in coastal seacliffs. Analyses of the geometry and kinematic indicators at the current exposure level strongly suggest that this part of the diapir intruded at a low angle to form an inclined sill or dyke-like body at least 0.5 km in diameter. Microstructural analysis indicates a zonation of deformational features between the core and margins of the diapir resulting from an evolving series of fabrics and the increasing concentration of strain towards the margins. Specifically, we interpret early independent particulate flow (IPF) fabrics as indicating deformation in a low effective stress environment with the possibility of turbulence during initial mobilization and intrusion. The subsequent transition to cataclastic flow indicates deformation occurring in the presence of increasing effective stress, and the creation of broad marginal shear zones suggests strain hardening. The final transition to IPF fabrics limited to narrow strain softened marginal shear zone suggests decreasing effective stresses during the latest intrusion phase. In addition, the abundance of veining phases associated with the latter part of the intrusion history indicates that the diapir became a major fluid conduit for mineralizing fluids toward the end of its emplacement history.

INTRODUCTION

MUD diapirism can be a locally and regionally significant tectonic process. For example, abundant mud diapirs form large volumes of mélange in numerous convergent, transpressive and basinal–passive margin environments (Higgins & Saunders 1967, 1974, Gilreath 1968, Musgrave & Hicks 1968, Bishop 1978, Williams *et al.* 1984, Barber *et al.* 1986, Brown 1987, Brown & Westbrook 1988, Hovland & Judd 1988). Where present, mud diapirs are commonly associated with active tectonic structures (Ridd 1970, Barber *et al.* 1986, Breen *et al.* 1986, Brown & Westbrook 1988), overpressuring at depth and hydrocarbon generation (Kugler 1939, Hedberg 1974, Ridd 1970, Hovland & Judd 1988, Hovland & Curzi 1989, Brown 1990, Reed *et al.* 1990). In addition, mud diapirs and related sedimentary intrusive phenomena can form important conduits for fluids migrating out of low permeability sedimentary sequences buried by sedimentary or tectonic processes (Brown 1990, Westbrook & Smith 1983, Hovland & Curzi 1989, Henry *et al.* 1990, Le Pichon *et al.* 1990).

Despite their local and regional importance, most of the information on mud diapirism in convergent margin systems comes from remote geophysical observations (Breen *et al.* 1986, Brown & Westbrook 1988, Reed *et al.* 1990) and a small number of submersible studies (Le Pichon *et al.* 1990). There are relatively few studies of subaerially exposed regions of mud intrusions from which inferences on the internal structure and behavior of mud diapirs can be drawn (Williams *et al.* 1984, Barber *et al.* 1986, Pickering *et al.* 1988, Orange 1990). Our continued studies of the kinematic and microstructural development of an ancient diapiric mélange body (Rau & Grocock 1974, Orange 1990) exposed along the coastal Olympic Peninsula of Washington (Fig. 1) reveal that diapiric mélanges can show a complex evolution and spatial zonation in fabrics from the core of the diapir to the margin. Furthermore, mineralizing fluids became an

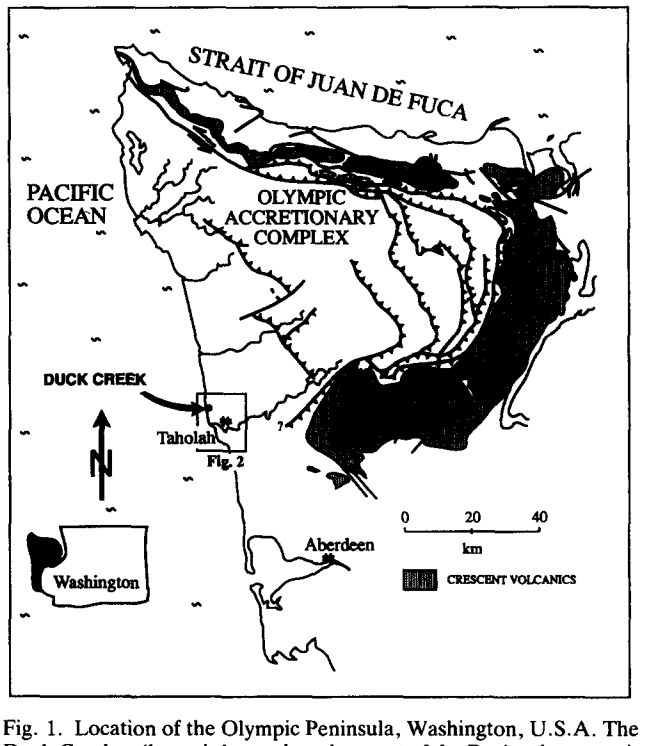

Fig. 1. Location of the Olympic Peninsula, Washington, U.S.A. The Duck Creek mélange is located on the coast of the Peninsula approximately 10 km north of Taholah, near the southern limit of the exposed Olympic accretionary complex (after Tabor & Cady 1978, Snavley & Kvenvolden 1988).

*Present address: Scripps Institution of Oceanography, University of California, La Jolla, CA 92093-0220, U.S.A.

increasingly important factor in the development of the mélange despite the expected relatively low intrinsic permeability of the mud composing it. Indeed, the diapir apparently provided an important pathway for fluid advection through the slope cover sequences from the Hoh accretionary wedge below.

We use inferences drawn from the changes in deformation mechanisms (Knipe 1986) and basic critical state concepts (Roscoe *et al.* 1958, Schofield & Wroth 1968, Atkinson & Bransby 1978, Jones & Addis 1986) to relate the temporal and spatial changes in fabrics and strain within the diapiric mélange to changes in strain and effective stress during intrusion. This information, together with the overall geometry of the mélange body, is used to infer a historical trajectory of the intrusion path in terms of depth, overpressuring and effective stress.

REGIONAL TECTONIC SETTING

The Duck Creek mélange is part of an accretionary complex composed of highly deformed Miocene to Eocene sedimentary sequences and a younger slope cover sequence. The deformed Hoh rock assemblage (Rau 1973), exposed along Washington's Olympic Peninsula coastline (Fig. 1), was accreted in Neogene time and uplifted by the Pliocene (Stewart 1970, Rau 1973, 1979, Tabor & Cady 1978, Snavely & Wagner 1982). The Hoh forms the onland continuation of the modern Cascadia accretionary complex where currently Miocene to Pliocene oceanic crust is being subducted beneath the western margin of the North American continent, at an azimuth of about 60° and a rate of 4 cm year^{-1} (Riddihough 1977). The uppermost Miocene to Pliocene Quinault Formation is a slope cover sequence that unconformably overlies the accreted rock of the Hoh (Rau 1973). The Quinault is exposed only in limited areas onland but is regionally extensive offshore; seismic and drilling data indicate that it is rarely more than 2–3 km thick (Rau & McFarland 1982, Snavely & Wagner 1982). The Quinault Formation is only mildly deformed by broad 25° E-plunging folds and widely spaced syn-sedimentary normal faults.

GENERAL GEOMETRY AND CONTACT RELATIONSHIPS OF THE MÉLANGE BODY

The Duck Creek mélange is exposed along the coastal cliffs of the Olympic Peninsula some 10 km north of Taholah (Fig. 2). This mélange occurs as a body some 550 m in N–S cross-section (Figs. 3 and 4). The initial mapping for this project was done on a photomosaic base map at a scale of 1:100 (Orange 1990). Internally the mélange comprises highly deformed and disrupted Hoh lithologies which have yielded middle Miocene fossils (Rau 1975, Orange 1990). Both the northern and southern contacts of the mélange dip inward at a moderate angle. To the north of the Duck Creek section, the Quinault Formation is comprised of thin turbidites, while to the south the Quinault occurs as thick-bedded coarse sandstone and conglomerate. This juxtaposition of different lithologies in association with the mélange

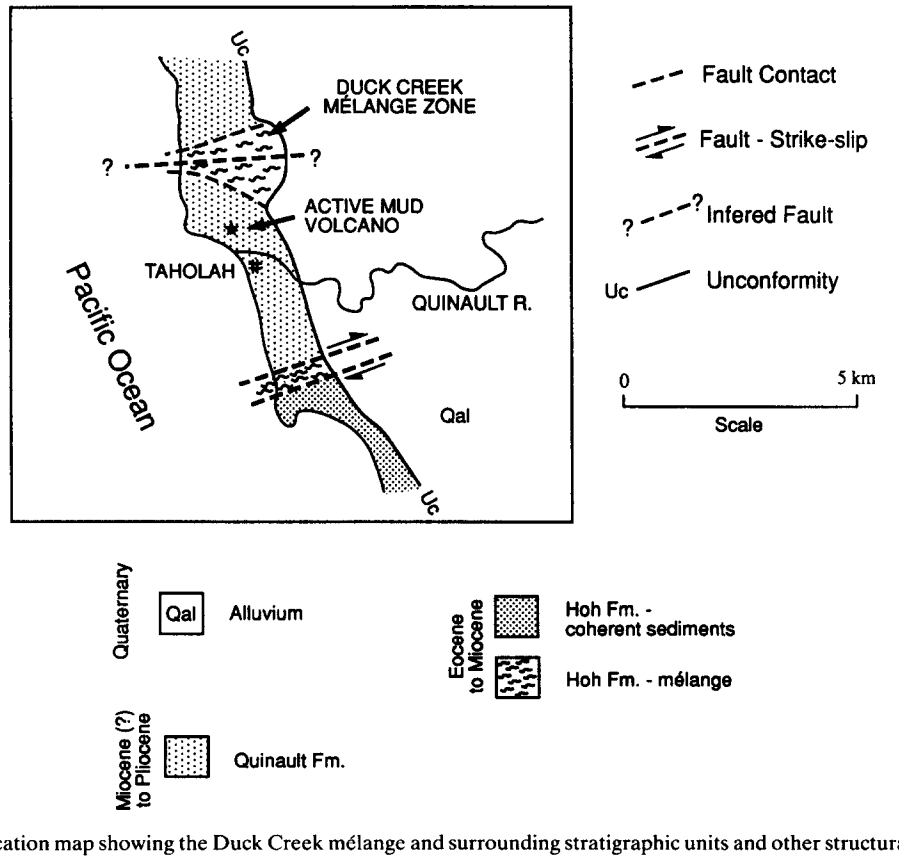

Fig. 2. Location map showing the Duck Creek mélange and surrounding stratigraphic units and other structural elements.

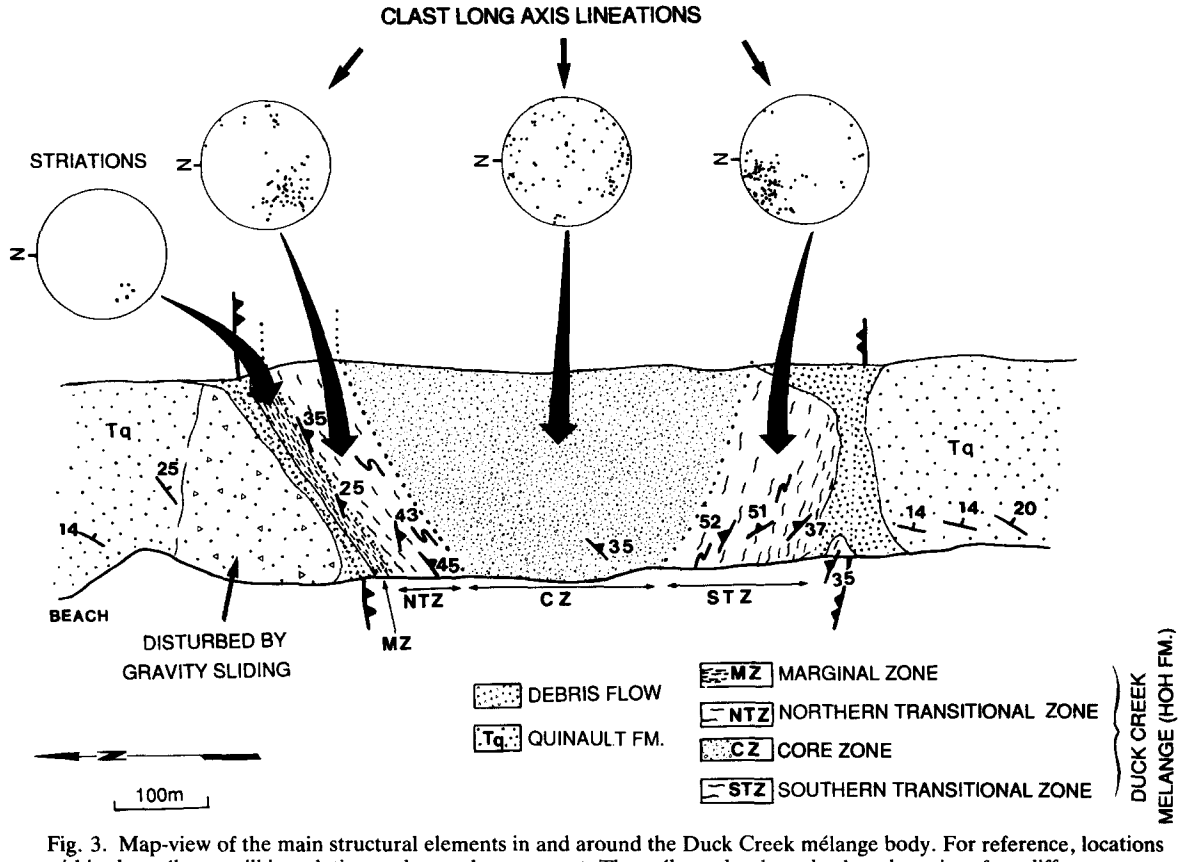

Fig. 3. Map-view of the main structural elements in and around the Duck Creek mélange body. For reference, locations within the mélange will be relative to the northern contact. The mélange has been broken down into four different zones based on lineation data (Orange 1990) and microstructure: the northern marginal zone (MZ), northern transitional zone (NTZ), core zone (CZ) and southern transitional zone (STZ). The southern marginal zone is obscured by slumping.

led Rau & Grocock (1974) and later Orange (1990) to propose that the Duck Creek mélange was a diapir intruding along a probable pre-existing normal fault in the Quinault slope cover sequences.

The mélange is generally well exposed but some recent slumping has resulted in a small (<10 m) exposure gap across the northern contact and some down slope displacement of otherwise undeformed Quinault Formation. A slightly larger exposure gap (50–100 m) occurs across the southern contact. In the following discussion we will refer to locations within the diapir relative to the northern contact and we will mostly refer to structural gradations across the better exposed northern margin to core transect of the mélange (Fig. 3). As far as we can ascertain very similar gradations also occur across the southern portion of the mélange.

Foliation in the mélange is manifested by a subparallel anastomosing scaly fabric in the mud matrix and a general block alignment in the foliation plane. The blocks are predominantly sandstone and siltstones with rare volcanic clasts. The scaly surfaces commonly have a highly polished sheen and are striated. The orientation of the foliation in the mélange near the margins, and the general map pattern (Figs. 3 and 4), indicate that the

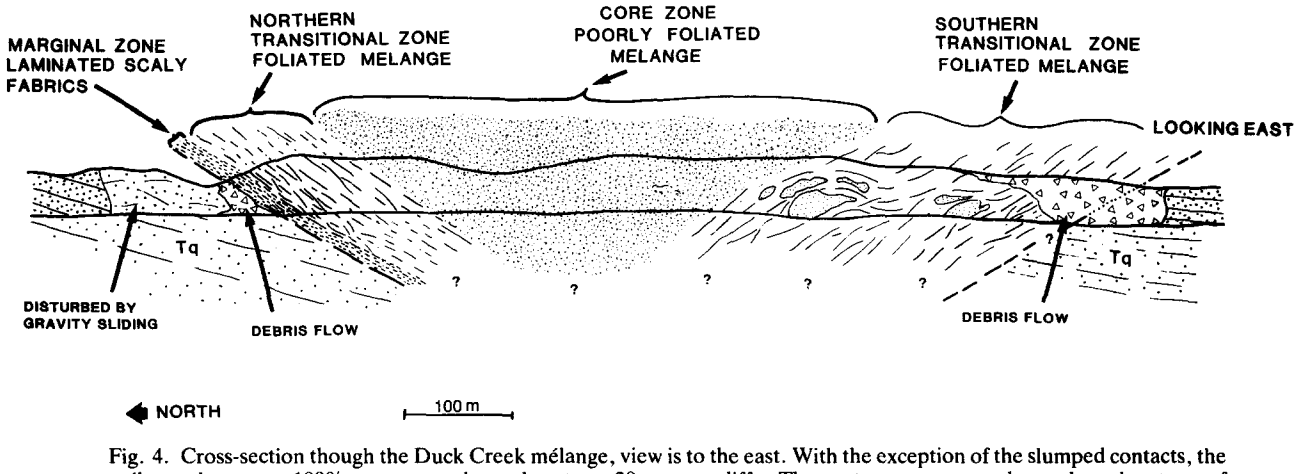

Fig. 4. Cross-section though the Duck Creek mélange, view is to the east. With the exception of the slumped contacts, the mélange has near 100% exposure along the steep 20 m sea cliffs. These steep exposures have the advantage of corresponding to a cross-section of the mélange.

north and south contacts of the Duck Creek mélange dip towards the center of the body at approximately 25–35°. The mélange, therefore, appears to be structurally emplaced into and over the surrounding Quinault Formation at this level of exposure. Any upper contact of the mélange with the Quinault is not preserved because the mélange is currently unconformably overlain by undeformed Pleistocene to Holocene glacial and terrace deposits.

The mesoscopic intensity of the foliation increases from the center to the north and south margins. Slightly off center in the mélange, between 100 and 300 m, is a core of poorly foliated to unfoliated material (Figs. 3 and 4). In this core region, scaly fabrics occur only as thin and restricted zones and consistent foliation orientations in general are elusive and enigmatic. Another feature of the Duck Creek mélange is the greater abundance of large blocks in this core region (Orange 1990). The block size distribution is, however, somewhat asymmetric with the peak in block size occurring slightly to the southern edge of the core zone.

The foliation becomes progressively better developed from south to north in this core zone (Figs. 3, 4 and 5a). Between 20 and 100 m from the northern contact we identify a transitional zone in which the spacing of scaly fabrics decreases and in which the foliation is highlighted by a number of layers rich in small sandstone boudins. Within approximately 20 m of the northern contact (Figs. 3 and 4), the mélange matrix develops an intense and almost planar scaly fabric with a shear zone spacing of less than 1 mm (Fig. 5b). This marginal laminated zone has a lighter weathering color and dips at approximately 080/25° to the southeast. We observe that the matrix in this marginal zone is far less indurated than the matrix elsewhere, and has a consistency of stiff clay in fresh exposures which have not dried out in contact with air. Occasional lenticular pods of more indurated diapiric material are preserved in the marginal zone.

On the south side of the core region (between 300 and 450 m), we observe a similar transitional zone, with the development of a crude layered foliation and more abundant scaly fabrics. This foliation increases in intensity towards the southern contact (Figs. 3 and 4) and dips at approximately 290/35° to the northeast. The southern contact, however, is obscured by slumping.

KINEMATIC INDICATORS

On the northern and southern margins of the mélange the general foliation dips inwards at moderate angles (25–40°) towards the core (Fig. 3 and 4). The following four types of kinematic indicators, when taken together, define movement vectors in the plane of this foliation: (a) striations on the scaly fabric surfaces; (b) fold orientations and vergences; (c) long axes alignments of clasts; and (d) local asymmetric tails of disaggregated material coming off blocks.

Striations on the scaly fabric surfaces appear randomly oriented throughout the mélange except in the marginal contact zone within 20 m of the northern contact (Figs. 2 and 3). In this marginal zone, striations are well developed (Fig. 5b) with a consistent plunge of 20–30° to the west-southwest (Fig. 3). Furthermore, within this region asymmetric boudins and folds (Orange 1990) in the scaly fabric give a top-to-the-east-northeast sense of motion on the slip surfaces, consistent with the striation orientations.

Orange (1990) studied clast long axes orientations in the mélange and found that within the northern marginal and transitional zones, most clast long axes clustered about a general SW plunge of between 15° and 35° (Fig. 3). Orange (1990) proposed the clasts in the mélange acted as rigid blocks in a ductiley deforming matrix with the long axes of more elongate blocks rotating under a combination of pure and simple shear so that, at a given time, most had orientations subparallel to the transport direction (Ghosh & Ramberg 1976, Freeman 1985). More detailed observations indicate that mechanical boudinage and disaggregation commonly tends to elongate clasts in the direction of transport, so that the clustering of the clast long axes are probably a result of both processes operating simultaneously. The clast long axes orientations are also consistent with the striation orientations on the scaly fabric surfaces in the northern marginal zone.

In contrast to the northern margin of the mélange, clasts in the core of the mélange body have long axes that exhibit close to a random pattern, although there may be some slight concentration around a low-angle N–S axis. No consistent fold orientations and geometries were identified in this zone, and no consistent striation orientations were observed. However, in the southern transitional zone, clast long axes again define a strong general lineation. The clast long axes plunge to the northwest at approximately 10–25° (Orange 1990). The few asymmetric folds in the southern transitional zone suggest motion up towards the southeast, consistent with the clast lineations.

In summary, strongly defined foliation and lineation patterns in the northern marginal and transitional zones are consistent with emplacement of the Duck Creek mélange up to the northeast at a shallow angle of between 15° and 35° relative to the Quinault wall rocks.

Fig. 5. (a) Foliation in the northern transition zone core of the mélange (north to left) approximately 30–50 m south of the northern contact. Foliation (f) dips from top left down to bottom right. (b) Hand specimen of the muddy laminated scaly matrix at the northern contact of the mélange showing lineation on shiny fracture surfaces. (c) Disturbed, discontinuous, convoluted laminations, and folding in a region of the core in which IPF fabrics are preserved (scale bar = 1 cm). (d) Complex cross-cutting calcite veins in the core region of the mélange (scale bar = 0.5 cm). (e) Scanning electron microscope (SEM) micrograph of a cataclastic shear zone in a sandstone block (location shown in Fig. 6a). Tops of sand grains (dark gray) have been polished. Z marks an individual large sand grain in the shear zone wall below which a broken grain (circled) can be seen (scale bar = 500 μm). (f) Enlarged SEM micrograph of the broken grain (B) shown circled in (e). FR-fracture in grain (scale bar = 200 μm).

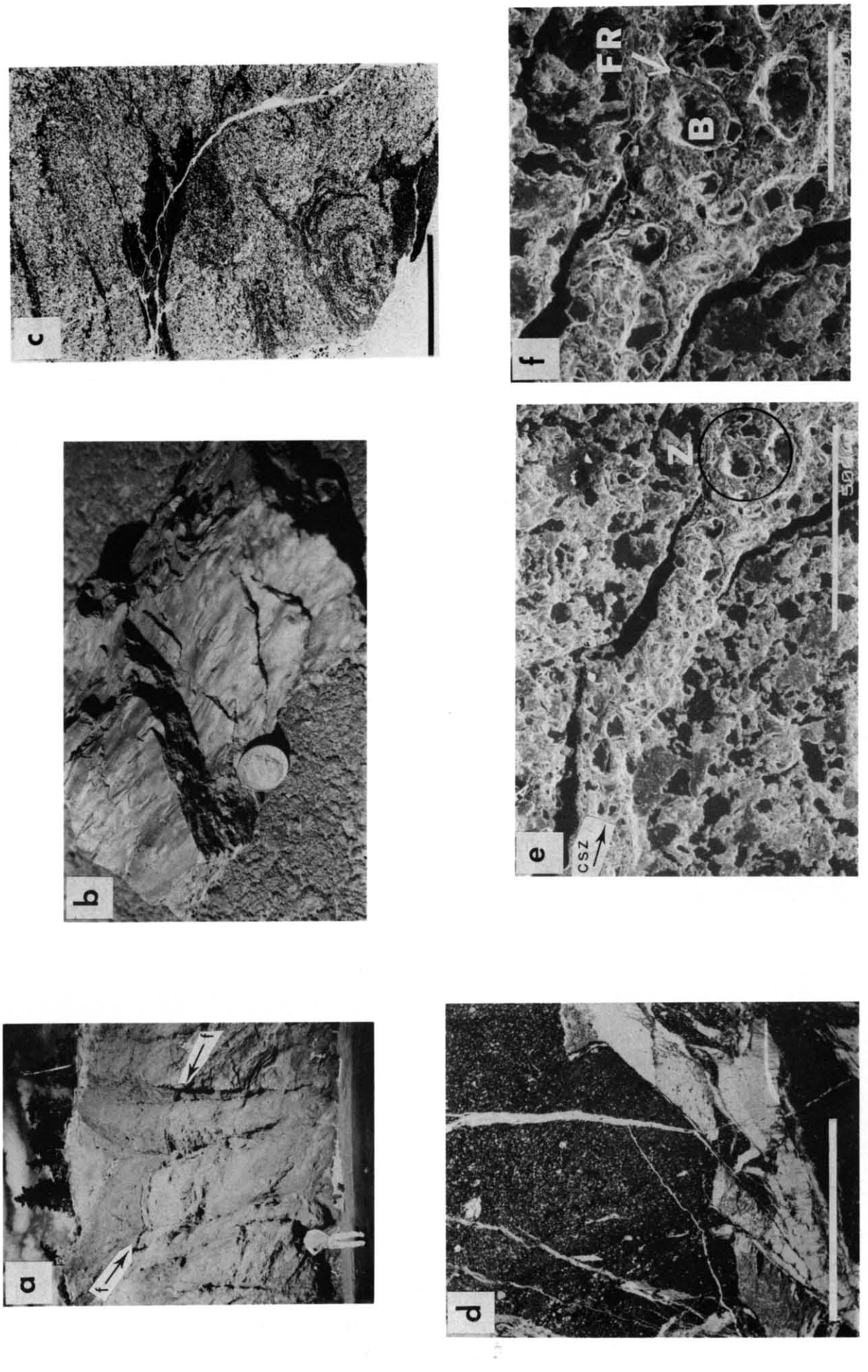

Fig. 5.

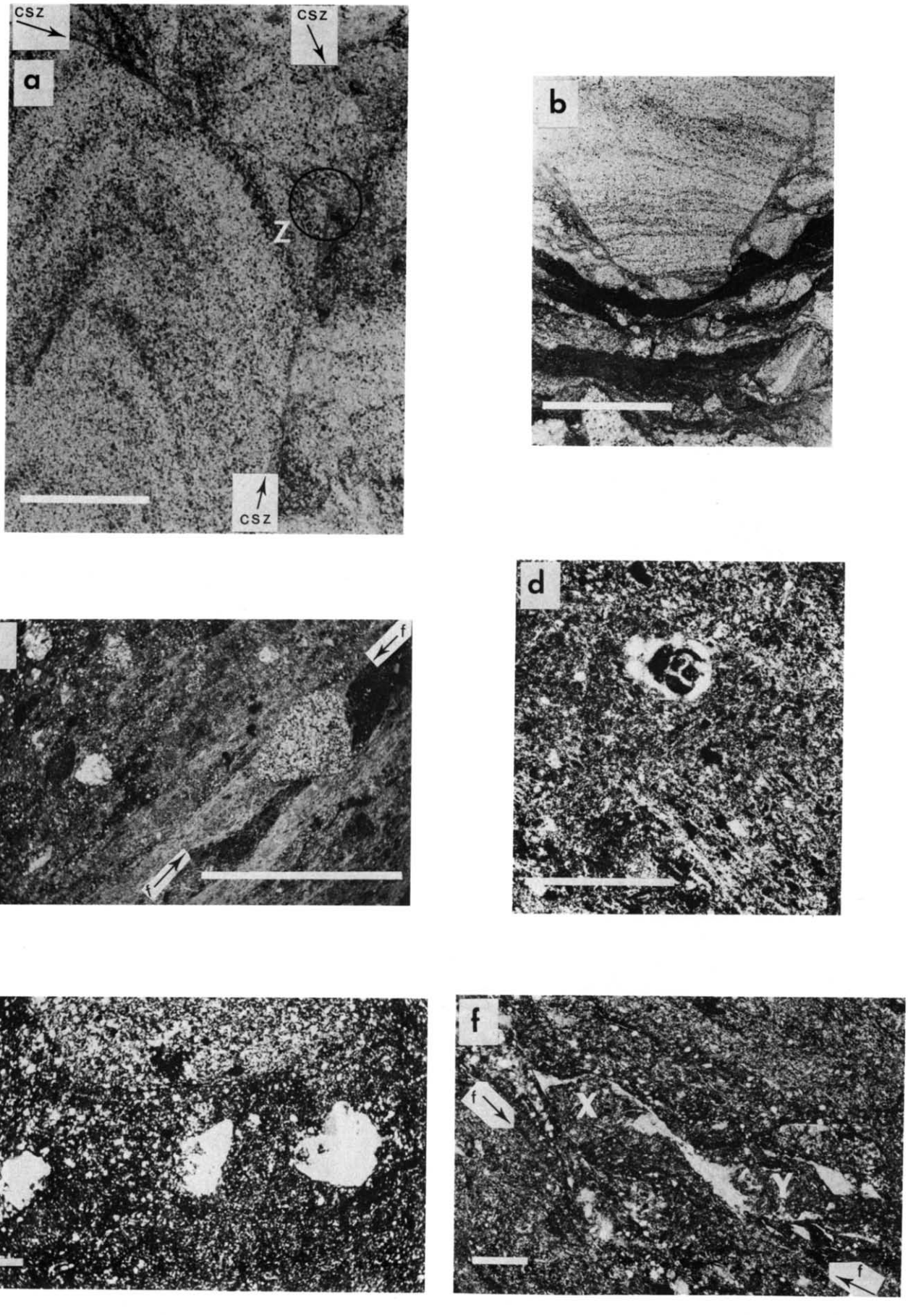

Fig. 6.

Similar observations at the southern transitional zone indicates emplacement up to the southeast at an angle of 5–25°. The poorly clustered to randomly oriented clast long axes and lack of consistent foliation in the core of the mélange suggest little consistent emplacement pattern in this zone.

ZONATION AND EVOLUTION IN MICROFABRICS

A suite of samples obtained on a transect from the core to the northern marginal zone of the mélange have been analysed to determine the microstructural evolution of the Duck Creek mélange. Based on the overall structural patterns described above and the microfabric associations we have divided the mélange into three domains with transitional contacts, which appear to be asymmetrically distributed about the core of the mélange.

Core zone (100–300 m)

In the core zone we observe poorly developed mesoscopic foliation in the mélange and little or no obvious deformation in over half the thin sections from this region. Benthic foraminifera are, for example, commonly preserved intact in the matrix. In the rest of the thin sections there is evidence that grain boundary sliding accommodated independent particulate flow (IPF) (Borradaile 1981, Knipe 1986) during the earliest phase of sandstone and siltstone block disruption. In more massive sandstones the principal evidence for IPF is the absence of any other visible manifestation of deformation, like grain breakage, by which block disruption and boudinage could have been accomplished. In siltstone and sandstone units, disruption and folding of sedimentary laminations within blocks (Fig. 5c) again appears to have been accommodated without any apparent grain breakage or grain size reduction. Where sandstones are locally cemented by calcite, however, we see little disruption of sedimentary laminations by IPF, perhaps signifying early carbonate concretion formation.

Although cross-cutting relationships are clearer in the transitional zone (see below), in the core region these IPF fabrics appear to pre-date continued boudinage accommodated by grain breakage along complex anastomosing cataclastic shear zones or web structure (after Byrne 1984). This cataclastic deformation is an intense but localized feature in the core zone in comparison to its widespread occurrence in the more marginal regions of the diapir. Discrete shear zones defined by well developed scaly fabrics in the mud matrix (as indicated by the alignment of optical axes in the clays and oriented patterns of brightly birefringent zones along shear planes) are generally not common except in the limited regions in which cataclastic features were observed.

Calcite veins are abundant in the core zone of the mélange, and appear to have experienced only limited deformation subsequent to formation. In the northern part of the core zone (between 100 and 150 m), calcite is found in association with minor quartz and zeolite. The zeolite is most likely to be laumontite, based on the abundance of this mineral in the local outcrops of the Hoh Formation (Stewart 1974). These minerals infill different veins in various orders although the zeolite appears most commonly as a late cavity filling phase, and as cross-cutting mono-mineralic veins. The more common earlier calcite veins occur as infillings of extensional fractures in sand and siltstone boudins, as en échelon sigmoidal vein arrays in the matrix, and as complex netted vein assemblages (Fig. 5d). Occasional inclusion trails testify to the episodic opening and infilling of veins. In the core zone we have noted only rare occurrences of calcite veins cut by pressure solution cleavage or shear zones. Where calcite veins are disrupted they appear to be associated with local cataclasis. We interpret the calcite and quartz veining to be a late syn-deformational feature of the local deformation sequence in the core regions, developing toward the end of the period of cataclasis. Where observed, the zeolite appears to be a late to post deformation feature in the core, as it generally cross-cuts any local deformation.

Northern transitional zone (20–100 m)

The main deformation in the transitional zone appears to be associated with cataclastic deformation within the sandstones (Figs. 5e & f). There is good local evidence, however, that the cataclastic fabrics postdate a phase of deformation and block disruption accommodated by IPF (as in the core). For example, Fig. 6(a) shows a ductile looking fold in a discontinuous disrupted laminated sandstone formed without any visible grain breakage. This fold is cut by later discrete cataclastic shear zones (CSZ in Fig. 6a), shown in greater detail in Figs. 5(e) & (f), in which grain breakage and grain size reduction is occurring. The early IPF fabrics, however, are less commonly preserved in the transitional zone than in the core zone perhaps due to a greater degree of cataclastic overprinting in the former. In the transitional

Fig. 6. (a) Ductile fold in the transitional zone that is cut by discreet cataclastic shear zones (CSZ). A portion (Z, circled) of one of these shear zones is shown in Figs. 5(e) & (f) (scale bar = 0.5 cm). (b) Pinch and swell structure accommodated by both localized and diffuse cataclastic flow in the transitional zone (scale bar = 1.cm). (c) Isolated ridged rounded blocks in heavily sheared mud of the laminated scaly fabrics in the marginal zone at the northern diapir contact (scale bar = 0.5 cm). Little to no evidence of block disruption associated with grain breakage can be seen in this marginal zone. Contrast this with the cataclastic fabrics and pinch and swell structure widely developed in the northern transitional zone (Figs. 5e and b above). Trend of shear zones marked (f). (d) Preserved foraminifera in the matrix of the laminated scaly fabrics (scale bar = 1 mm). (e) Embayed and dismembered calcite vein in the northern marginal shear zone (scale bar = 1 mm). (f) Sigmoidal pressure shadows that are associated with ridged blocks (x,y) are infilled by zeolite in the marginal shear zone (scale bar = 1 mm).

zone, foliation and deformation intensities increase toward the northern margin with some form of disruption observed in nearly all of the samples derived from this zone. Common pinch and swell structure leading to extension of sandstone blocks (Fig. 6b) is accommodated either by complex localized cataclastic shear zones or more distributed grain disaggregation and local grain breakage. Wisps and tails of broken disaggregated material coming off boudins become spread along shear surfaces in the muds giving rise to ductile looking textures (Fig. 6b).

In the transitional zone, calcite veins in boudins cut, and are cut by cataclastic shear zones. The calcite veins also tend to be oriented perpendicular to the local extension direction of the boudin (Orange 1990). Calcite vein material is also observed as disrupted fragments in the mélange matrix. Only in rare instances are calcite veins observed to cross-cut the scaly foliated mud matrix of the mélange. Disrupted calcite veins are observed in at least 50% of the boudin samples, and as many as 90% of the matrix samples. Zeolite veins are also abundant in this zone. In some instances, these veins are offset by shears in the matrix, yet they also infill voids formed by tension gashes and block rotation in the matrix. Most importantly, much of the zeolite occurs as undeformed veins along dilated matrix shear surfaces, as well as in veins that cross-cut the matrix fabric.

From these observations, we interpret that the main phase of calcite vein formation occurred after the phase of IPF, coevally with the main episode of cataclasis, and that it was post-dated by significant continued matrix deformation. The zeolite (probably laumontite, after Stewart 1974) appears to have begun to be deposited syn-deformationally during the phase of cataclasis in the transitional zone, but continued to be deposited after significant deformation ceased in this zone. In the field, the light weathering zeolite gives the normally dark grey shear and fracture surfaces a prominent piebald weathering pattern when exhumed.

Northern marginal zone (0–20 m)

Although the 10 m nearest the northern contact are not exposed, the remaining exposure from 10 m south is excellent and a distinctive range of fabrics are seen in association with the intense laminated scaly fabrics of this marginal zone (Figs. 3, 4 and 5a & b). In this region many of the competent inclusions have a highly rounded equant geometry and appear to be behaving as rigid rotating inclusions in the highly sheared matrix (Fig. 6c). Cataclastic fabrics are observed only locally, preserved in lenticular pods of indurated transitional zone material. Pinch and swell structure is uncommon outside these pods in contrast to the transitional zone where pinch and swell structure and cataclastic deformation is intense. Significantly, undeformed foraminifera also occur in the matrix of the marginal zone (Fig. 6d) even though there is abundant local evidence, in the form of anastomosing shear zones, that the deformation in this matrix is relatively intense. This part of the diapir is also poorly indurated and soft (having a stiff leathery clay consistency so that sheets can be bent by up to 30° without breaking and in which a hammer can be embedded) in contrast to the more central zones where the more indurated mud behaves brittley.

All of the calcite veins in the marginal zone occur as highly disrupted fragments. In addition, calcite vein fragments in the matrix have a highly embayed or fretted morphology and appear corroded (Fig. 6e). Zeolite occurs as a common syndeformational veining phase in this marginal zone, occurring both as infillings in pressure shadows that develop around rigid clasts in the matrix (x and y in Fig. 6f) and as small concretions.

The lack of any obvious intense cataclasis, the survival of intact foraminifera, coupled with the intense scaly foliation and soft clay consistency, suggest the main deformation mechanism in the marginal zone was different to the one operating in the transitional zone. Although the complex history of the materials in the marginal zone makes it difficult to demonstrate conclusively that the latest deformation was accommodated by IPF, we suggest that this mechanism is most consistent with the above mentioned observations. The intense deformation appears to post-date calcite deposition. In contrast, zeolite deposition appears as a largely syn-deformational feature.

DISCUSSION: THE DUCK CREEK MÉLANGE AS A DIAPIR

General geometry and emplacement

Offshore seismic data indicate that mud diapirs with source regions in the accreted Hoh sequences and vertical dimensions of at least 2 km pierce the lower portions of the Quinault slope cover section in the offshore regions of the Washington coast (Rau & Grocock 1974, Snavely & Wagner 1982, McClellan & Snavely 1987, Rau 1987). In the exposed Duck Creek mélange, Hoh lithologies are similarly emplaced as a cross-cutting body in the stratigraphically overlying Quinault sequence (Rau & Grocock 1974, Orange 1990). However, the emplacement patterns of the Duck Creek are not those of a simple vertically intruded diapir. The kinematic indicators instead indicate that the mélange was intruding obliquely upwards to the east at an angle between 10° and 35°. In addition, the movement vectors diverge across the mélange rising up to the northeast near the northern contact and up to the southeast at the southern contact. The Duck Creek mélange is interpreted to be an obliquely intruded mud diapir that was spreading laterally at this level of exposure.

In Fig. 7(a) a schematic three-dimensional model for the geometry and dynamics of the Duck Creek Diapir is presented. The three-dimensional representation is based on the general diapir–wall rock contact outcrop patterns, and main internal foliation geometries, and the diverging slip vectors near the northern and southern contacts. We propose the diapir is an obliquely intruded

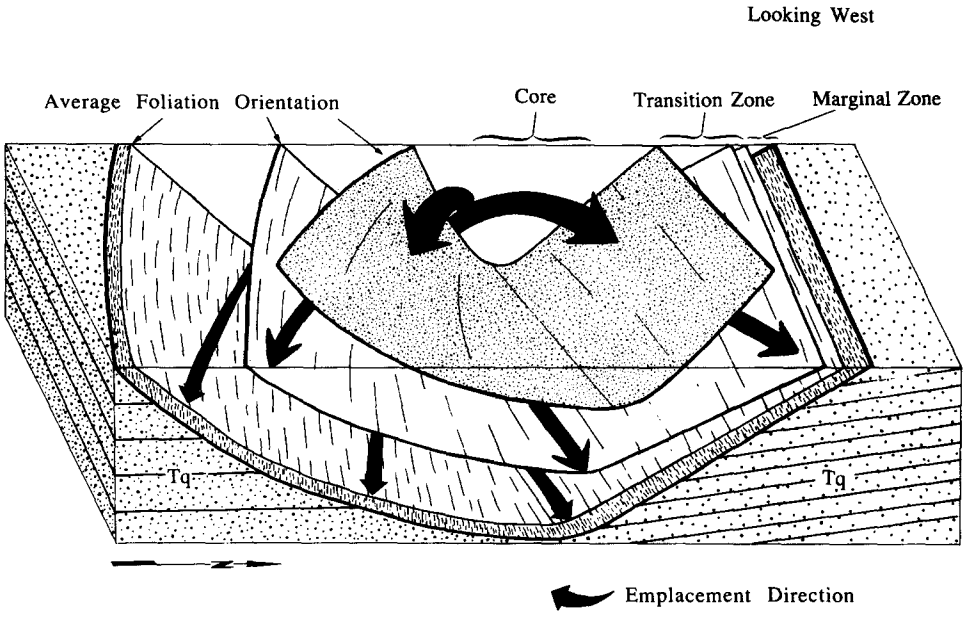

Fig. 7. Three-dimensional model for the general geometry and emplacement of the Duck Creek Diapir at its current exposure level. Tq is the Quinault Formation. Stipple on foliation surfaces marks strike line orientation; the lineation and emplacement direction are parallel to large arrows.

lenticular shaped body that widens to the east. The N–S component of expansion required by the diverging slip vectors (Figs. 3 and 7) may have been accommodated by some sub-vertical flattening and extension perpendicular to the eastward transport direction. Although the long complex deformation history makes it difficult to conclusively demonstrate, this perhaps accounts for the poorly developed low-angle N–S alignment of the blocks in the core of the mélange (Fig. 3).

The Duck Creek Diapir represents a sill or inclined dyke originating from a major conduit to the west, seaward of the current exposures (Fig. 8). Perhaps, the Duck Creek Diapir mushroomed at the currently exposed level in the Quinault Formation because its density became greater than the surrounding shallow Quinault slope sediments. A possible example of a mud intrusion of similar geometry as proposed for the Duck Creek Diapir is shown in Fig. 9. This seismic reflection section shows a number of lenticular sills intruding the slope cover sequence surrounding a mud volcano in the Barbados Ridge complex (Brown & Westbrook 1988).

Rau & Grocock (1974) pointed out that, based on the differences in the facies in the Quinault Formation on either side of the mélange body, the Duck Creek Diapir appears to have intruded along a pre-existing (and currently obscured) fault with a probable normal displacement. As Behrmann (1991) has recently reminded us, it is considerably easier to propagate a vertical hydrofracture (or diapir) in an environment where the horizontal stresses are less than the vertical stresses and, thus, the diapir's spatial, and perhaps temporal, association with an extensional structure seems reasonable. The exact timing of emplacement of this diapiric body is not known. However, its position in the middle of the Pliocene Quinault section and the overlying Pleistocene–Quaternary unconformity (WNP-3 1986) suggests a mid to late Pliocene age. A locally active mud volcano indicates that similar processes may even be operating on a smaller scale today (Fig. 2).

Temporal changes in deformation mechanisms during intrusion

Our microstructural work shows that fabrics and deformation mechanisms accommodating the intrusion of the Duck Creek Diapir evolved with time. Three general stages of deformation are identified based on cross-cutting relationships (Fig. 10). Although we separate them out for descriptive purposes, these three stages

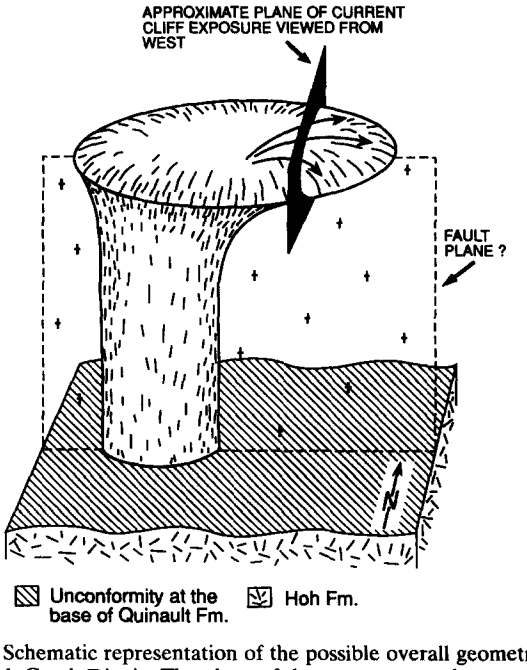

Fig. 8. Schematic representation of the possible overall geometry of the Duck Creek Diapir. The plane of the current coastal exposure is depicted. The diapir intruded up a pre-existing plane of weakness formed by a fault and apparently spread laterally pushing aside the low density Quinault slope sediments in the near surface.

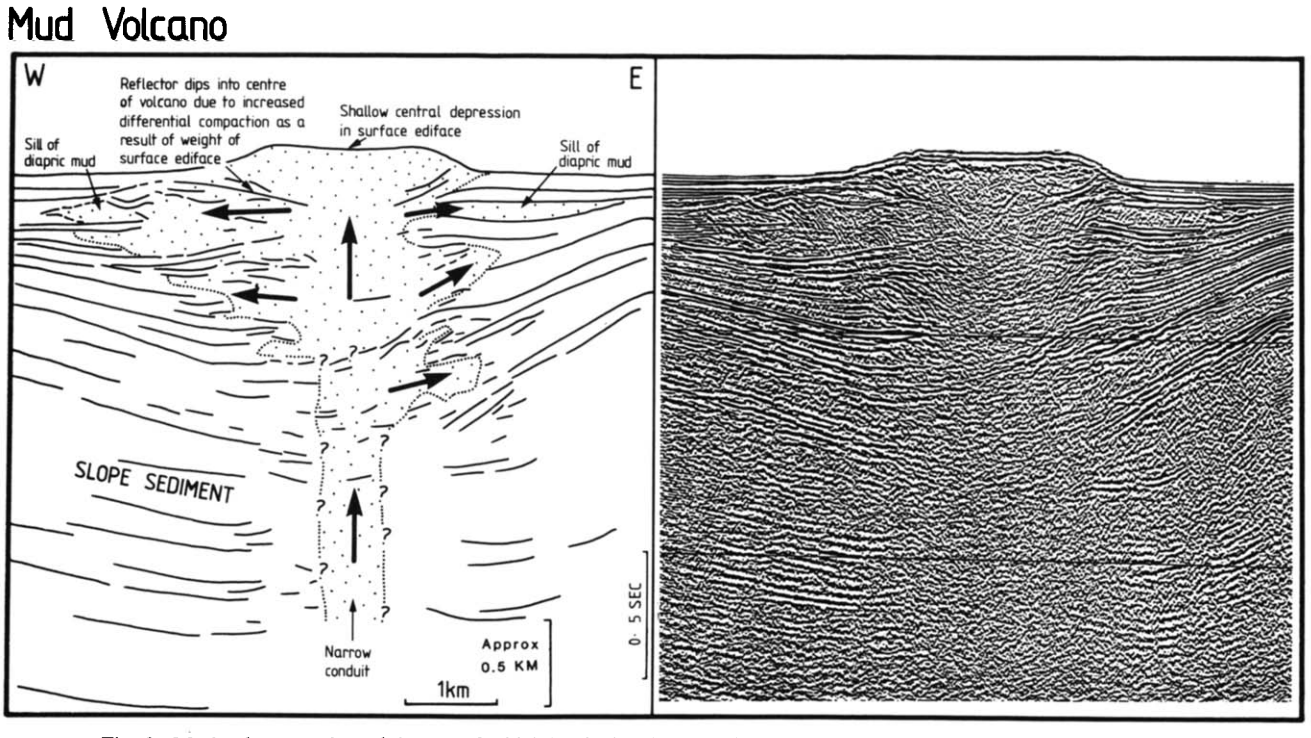

Fig. 9. Mud volcano and conduit around which lenticular sills intrude the slope sediments of the Barbados Accretionary Wedge (after Brown & Westbrook 1988). This may be an analog for the geometry of the Duck Creek Diapir.

probably form part of an evolving spectrum of behavior developed during a continual intrusion event (although they may be partly diachronous from the core to the margins). Early intrusion (Stage I) was accommodated predominantly by independent particulate flow. The middle period of intrusion (Stage II) involved intense cataclastic deformation in the broad outer region of the diapir and was associated with calcite, quartz and minor zeolite veining. The latest period of intrusion (Stage III) was accompanied by independent particulate flow and continued zeolite deposition (but no calcite deposition), with significant deformation limited to the diapir contacts. Zeolite deposition appears to have continued after the diapiric material was emplaced with dilatant scaly fractures becoming prime fluid conduits.

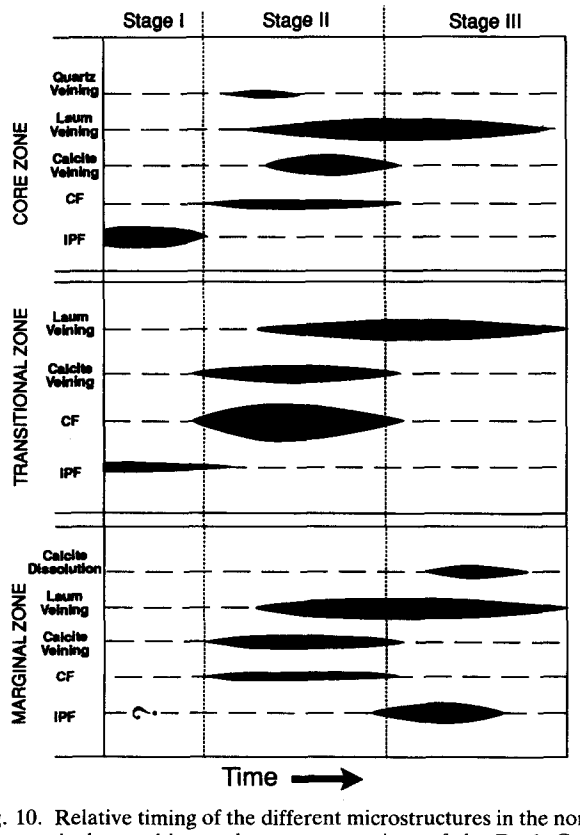

Fig. 10. Relative timing of the different microstructures in the northern marginal, transition and core zone regions of the Duck Creek mélange. Similar lateral changes are observed across the exposed portions of the southern margin of the diapir. CF = cataclastic floor.

The abundant veining toward the latter periods of intrusion suggests that the diapir became an increasingly important conduit for mineralizing fluids through fracture controlled conduits. The change in the veining phase compositions also indicates fluid chemistries and/or environmental conditions changed so that calcite (with minor quartz) dominated the period of cataclastic deformation (Stage II) with zeolite deposition taking over subsequently. The dilated scaly fabric in the mélange matrix appears to have been a particularly important route for zeolite depositing fluids toward the end of the diapirs history. The locally developed crack–seal textures and syn-kinematic relationships of the veins indicates that the fluid pressures probably fluctuated during intrusion causing repeated dilation of veins.

Changes in strain patterns across the diapir during intrusion: development of zonations in the diapir

Although a similar fabric evolution occurred throughout much of the diapir, there are important changes in the intensity and preservation of the different fabric elements from the core to the margins (Fig. 10). The

early IPF fabrics are best preserved in the core, are highly overprinted in the transitional zone, and appear to be absent or completely overprinted in the marginal zone of laminated scaly fabrics. In contrast, the later cataclastic fabrics are only locally developed in the core, are intensely developed in the transitional zone, but are overprinted in the marginal zone by the later phase of IPF. The later IPF fabrics are confined only to the margins. In addition, calcite veins are progressively more disrupted and overprinted by later and later phases of deformation towards the margins of the diapir. Observations of clast size and character further suggest that total strains may increase towards the diapir margins. For example, large intact sandstone and siltstone blocks are more commonly preserved in the core (Orange 1990). At the margins, clast rich layers appear to represent the highly strained and boudinaged remnants of similar large blocks.

Based on the above observations and inferences, we propose that active deformation became progressively concentrated towards the margins of the diapir during intrusion. During the earliest phase of intrusion deformation occurred throughout the diapir, but eventually developed a plug-like flow profile with narrow marginal shear zones. Similar narrow 'marginal gouge zones' have also been reported from drilling operations in mud diapirs in the Gulf Coast (Musgrave & Hicks 1968). It is this decreasing width of the marginal shear zones coupled with the evolution in deformation mechanisms that results in the apparent fabric zonation in the diapir. The preserved kinematic patterns in the mélange also suggest that the style of emplacement changed with time. Where early IPF 'soft-sediment' fabrics (Maltman 1984) are preserved in the core of the diapir there is little consistent pattern to the foliation or long axes patterns of the blocks, suggesting the early intrusion (Stage I, Fig. 10) of the diapir occurred in a fairly turbulent manner. In contrast, the increasing clast, foliation, and movement vector alignment related to the later periods of cataclastic and IPF fabric development, suggest a less turbulent pattern of emplacement during the later Stages II and III (Fig. 10).

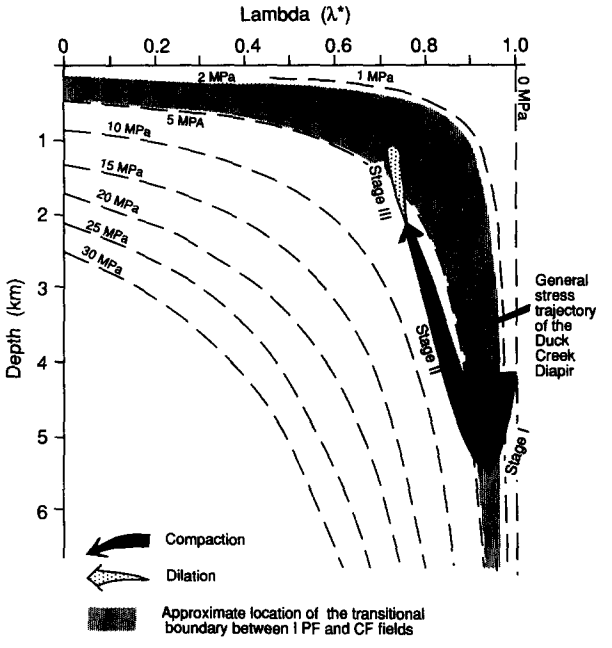

Fig. 11. Effective stress contours on a plot of λ^* vs depth (after Brown 1990). A possible general trajectory for the Duck Creek Diapir is marked. The approximate position of the minimum effective confining stress that marks the transitional boundary between independent particulate flow (below 1–5 MPa) and cataclastic deformation (above 1–5 MPa) in sheared sandstones is also marked, along with the suggested position of the three intrusion stages. Although fabrics in the sandstone blocks give information on the general trend of the effective stress changes, it is the muddy matrix that essentially controls the behavior of the diapir. The transitional boundary between IPF and cataclastic floor (CF) in the sandstone blocks does not necessarily exactly correspond to the onset of compaction and dilative episodes in the enclosing muddy matrix (the latter are denoted by the sense of widening and narrowing of the arrows).

EFFECT OF VARYING STRESS TRAJECTORIES ON THE EVOLUTION OF THE DUCK CREEK DIAPIRIC MÉLANGE

The Duck Creek Diapir's complex evolutionary history ultimately lead to the development of a zoned distribution of fabrics. We propose that the observed zonation is a product of changes in effective stress during the intrusion of a body of saturated porous sediments. These changes resulted in the evolution of the physical properties of the mud, deformation mechanisms in the sandstones, and patterns of strain across the diapir (Atkinson & Bransby 1978, Jones & Addis 1986, Karig 1986, Knipe 1986, Moore & Byrne 1987).

The effective stress trajectory that diapiric material can follow during intrusion depends on the change in the relative magnitudes of overburden load and internal fluid pressure. Both will change with depth. Fluid pressures in the diapir may be conveniently described using λ^*, the excess pore pressure ratio. The parameter λ^* represents the ratio of excess fluid pressures to the sediment overburden pressure (Shi & Wang 1988). In the case of a diapir:

$$\lambda^* = (P_f - P_{hydro})/(P_{dip} - P_{hydro})$$

so that

$$\lambda^* = 1 - \sigma'/(P_{dip} - P_{hydro}),$$

where P_f is fluid pressure in the diapir, P_{hydro} is hydrostatic pressure, P_{dip} is total average confining pressure exerted on the mud in the diapir by the overburden, and σ' is effective stress in the diapir. Figure 11, adapted from Brown (1990), depicts contours of effective stress on a plot of λ^* vs depth for a lithostatic gradient of 22.52 kPa m^{-1} (1 psi ft^{-1}). As the fluid pressure in the diapir cannot fall below the hydrostatic gradient, or greatly exceed the overburden pressure, λ^* of 0.0 and 1.0 are the approximate boundary limits of the diapiric system.

Although we have insufficient data to fully constrain the stress trajectory of the Duck Creek we do have enough data to say something about its general form. To place an approximate general stress trajectory for the currently exposed Duck Creek diapir in the framework of Fig. 11 we need boundary limits for the vertical

intrusion path and some idea of the effective stress changes during intrusion.

A minimum vertical displacement for the Duck Creek mélange can be roughly constrained using its geometrical position in the Quinault Formation. From measured sections along the coast (Rau 1970) it can be estimated that the mélange at its present exposure level is emplaced about 1 km up into the Quinault from the basal unconformity (Fig. 8), thus constraining the minimum vertical travel path for the diapir. As the Quinault Formation was probably not much more than 2 km to perhaps 3 km thick in this region (Snavely & Kvenvolden 1988), minimum paleo-source depth and emplacement levels of the diapiric material are, thus 2–3 and 1–2 km, respectively. Some idea as to the maximum paleo-source depth can be estimated from the thermal maturity of the mélange. Preliminary vitrinite reflectance data indicate that an angular mudstone clast in the northern transitional zone of the diapir had a reflectance of Ro = 1.23 (M. Underwood written communication 1988; $T \sim 220$°C; temperature correlations after Price 1983), while the highly strained marginal matrix material had a Ro = 0.68 (~140°C). In contrast, the Quinault wall rocks had a vitrinite value of Ro = 0.35 (45–50°C). If we assume a thermal gradient of 25°C km^{-1} (the present-day gradient is approximately 26°C km^{-1}; Snavely & Kvenvolden 1988), then this portion of the diapir may have originated at a paleo-source depth of as much as 6–9 km, and was emplaced within the Quinault Formation at a paleo-depth of approximately 2 km.

A number of different effective trajectories are possible for the mélange because fluid pressure (P_f) and total confining pressure (P_{dip}) can vary separately (with the former depending on the hydrogeologic system in and around the diapir). Without information on the absolute magnitude of paleo-stress and pore pressure during emplacement we cannot fully constrain the effective stress conditions in the Duck Creek Diapir. However, important limits can be placed on the general form of the stress trajectory by determining the trends in environmental conditions necessary to produce the observed evolution and spatial variation in microfabrics, as well as the apparent change in physical properties across the diapir.

The relative environmental conditions necessary for the main types of deformation mechanisms that can occur in sedimentary materials can be plotted in three-dimensional lithification (porosity and cementation), strain rate and effective stress space as is shown in Fig. 12 (after Knipe 1986). In the Duck Creek Diapir independent particulate flow and cataclastic flow (CF) appear to be the major deformation mechanisms accommodating intrusion.

As IPF fabrics are limited to low effective stresses (Borradaile 1981, Knipe 1986) and low states of lithification (Fig. 12), the early period of deformation (Stage I) must have occurred at low effective stresses. Fluid pressures must have remained very high for the source regions to have been buried deeply and yet have retained a relatively low state of compaction and low density with respect to the overburden sequence. We have put a portion of the burial path on the trajectory of the Duck Creek Diapir on Fig. 11. This burial path must exist because the source regions of the diapir must have been buried before the inception of diapirism (or the diapir must have been intruding upwards too slowly to keep up with the sedimentary or tectonic burial rate).

The effective stress must have subsequently increased (Fig. 11) in order to later drive the system from initial IPF (Stage I) towards increasing conditions of lithification and the CF field (Stage II, Figs. 10 and 12). We propose that the effective stresses must have fallen again at the end of the intrusive process (Stage III, Fig. 11) to account for the reversal in deformation mechanisms from CF (Stage II) back to IPF again (Stage III, Figs. 10 and 12).

Knowing, even very approximately, the effective stress conditions that form the boundary between the independent particulate flow and cataclastic fields (Fig. 12) would greatly help constrain the position of the stress trajectory of the Duck Creek Diapir on Fig. 11. As the average effective stress condition required for grain breakage will vary with such factors as porosity, grain size, cementation and strain rate (Knipe 1986, Zhang *et al.* 1990), we expect the boundary to be a transitional one. Studies like those of Zhang *et al.* (1990) indicate that the minimum critical average effective stress for microcracking and grain crushing in medium to fine sands under hydrostatic conditions are affected by porosity and can be as high as 75–380 MPa (porosities of 35 and 21%, respectively), while Zoback & Byerlee (1976) found that Ottawa sand (with a porosity of 31%) underwent grain crushing at effective average confining pressures of as low as 50 MPa. In general, however, experiments show that the average effective confining stress at which grain crushing and cataclasis are initiated

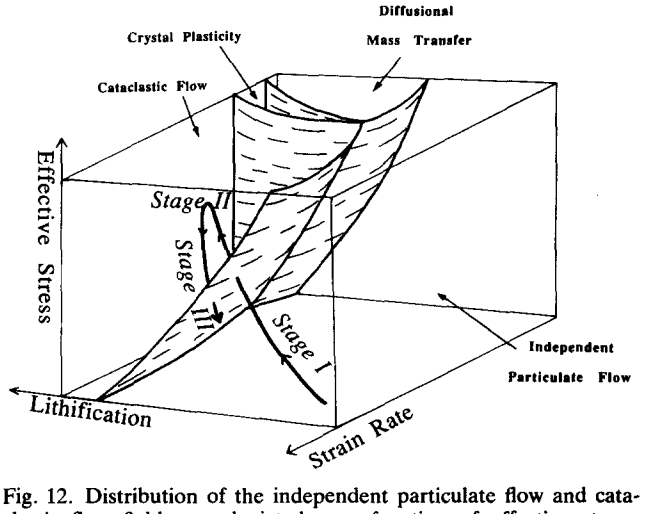

Fig. 12. Distribution of the independent particulate flow and cataclastic flow fields are depicted as a function of effective stress, lithification and strain rate (after Knipe 1986). Note that increasing lithification corresponds to decreasing porosity and increasing cementation. The proposed trajectory of the deforming sandstone blocks in the Duck Creek Diapir are marked. While the crystal plastic (CP) and diffusional mass transfer (DMT) fields are also marked, they seem to be mechanisms of only minor importance in the evolution of the Duck Creek mélange.

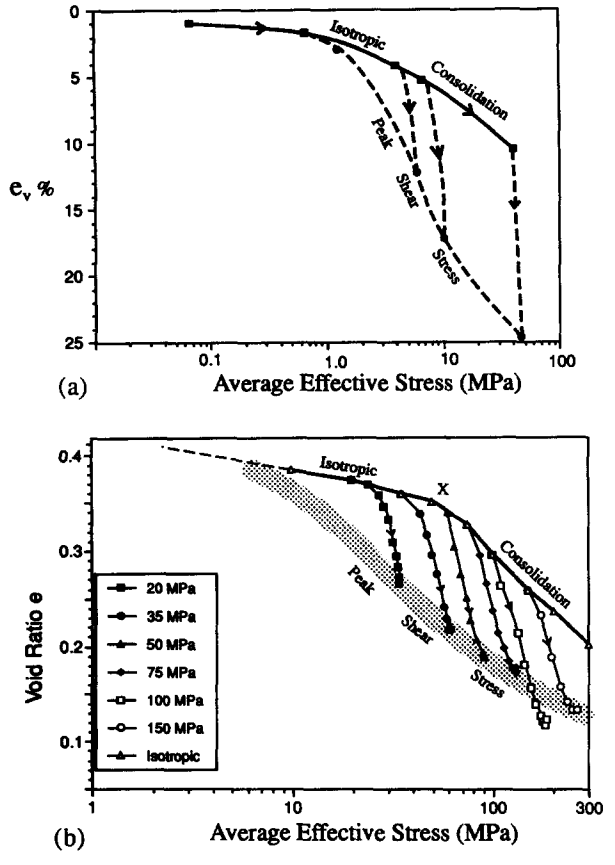

Fig. 13. (a) Influences of shear stress on volume changes associated with crushing of sand grains adapted from Bishop (1966). Average effective stress ($(\sigma_1' + \sigma_2' + \sigma_3')/3$) plotted against volume change. The sheared Ham River sand samples undergo appreciable grain crushing and further volume reduction over that observed in isotropically consolidated samples except at low confining stresses (<1 MPa). (b) Data from Zoback & Byerlee (1976) from deformed Ottawa sand. The data is reworked (after the style of Bishop 1966) to show void ratio change against average effective stress for isotropically consolidated and sheared samples. X marks the onset of cataclasis in the isotropically consolidated sample. The effective confining stress for each of the sheared samples is shown. An extrapolation (stippled line) of the void ratios at the peak shear stress suggests that grain crushing becomes significant during shearing of Ottawa sand at average effective confining stresses above 3–7 MPa (depending on the form of extrapolation used). The main thrust of our argument is that the onset of grain breakage occurs at relatively low effective confining stresses in sheared sands.

is substantially reduced as the deviatoric stresses increase. Handin *et al.* (1963), Zoback & Byerlee (1976), Logan & Rauenzahn (1987) and Morrow & Byerlee (1989) all found that cataclasis was significant in sandstones sheared and failed at average effective confining stresses above 15–25 MPa. Indeed, experimental results presented by Bishop (1966) and shown in Fig. 13(a) indicate that limited amounts of cataclasis may begin at average confining pressures as low as 0.7–1.4 MPa in sands with porosities of 41%. This relatively low average effective confining stress for the initiation of small amounts of cataclasis appears to be also borne out by the work of Zoback & Byerlee (1976). Figure 13(b) is a re-evaluation of some of the results of Zoback & Byerlee (1976) in terms of average effective stress vs void ratio. A similar extrapolation to that used by Bishop (1966) (see Fig. 13a) suggests cataclasis in Ottawa sand (Fig. 13b) may begin at confining pressures as low as 3–7 MPa (depending on the form of the extrapolation chosen).

In naturally deformed examples, relatively intense cataclasis was observed at the base of submarine slides coming off the lower trench slope of Mexico (Lucas & Moore 1986) at a depth below the sea floor of 230 m. Even at hydrostatic fluid pressures the mean effective confining pressures is unlikely to have been more than 2 MPa at this depth. In addition, Larue & Hudleston (1987) reported (and our observations have also confirmed) that a limited amount of cataclasis occurred at the base of the subaerially exposed Portuguese Bend landslide (Los Angeles, California) in medium- to fine-grained sandstones. This slide varies in thickness but is little more than 80 m in its deepest part and has a density of approximately 2000 kg m^{-3}. Even if the water table was below the level of the slide plane the maximum normal load on the base was probably less than 1.6 MPa.

In summary, experimental and natural examples suggest that a reasonable transitional boundary between the IPF and CF fields might lie somewhere between 1 and 5 MPa for medium to fine sandstones deformed with initial porosities between 31 and 41%. Consequently, we suggest the effective stress during the early period of IPF in the Duck Creek Diapir was probably at or below this level. In order to achieve these low effective stresses at depths exceeding 2 km, the pore pressure must have been greater than a λ^* of 0.8–0.9 (Fig. 11). The apparent change to IPF suggests the stress trajectory might again have crossed the CF–IPF boundary during the final stages of intrusion (Fig. 11). The greatest effective stress encountered by the diapir during the period of cataclasis is not known. Mud diapirs intersected by boreholes do, however, tend to be highly overpressured, with fluid pressure to overburden ratios of above 0.8 being common (Gilreath 1968, Ridd 1970). Thus, we feel it is reasonable to assume the stress trajectory was restricted to the relatively high pore pressure region of Fig. 11 and that effective stresses never rose to very great levels.

The strain and physical property variations across the diapir margins are also consistent with this pattern of changing effective stress. While fabrics in the sandstone clasts give information about the evolution of the stress environment, it is the properties of the muddy matrix that exerts the principal control on the behavior of the diapir (particularly when the clast density is not great). The relationship between the change in porosity, effective stress, and shear strength has been described in some detail for uncemented sediments in terms of 'critical state soil mechanics' and is beginning to be applied to many geological systems (Roscoe *et al.* 1958, Schofield & Wroth 1968, Atkinson & Bransby 1978, Jones & Addis 1986, Karig 1986, Moore & Byrne 1987). In shear zones undergoing active failure in their critical state the following three types of evolutionary change can occur in muddy unlithified sediments depending on how effective stress varies: (a) under increasing effective stress conditions deformation will lead to a progressive reduction in porosity, and an increase in shear strength. Strain hardening of muddy shear zones promotes the

migration of strain into the weaker surrounding material and consequent widening of the shear zones (Moore & Byrne 1987); (b) deformation under decreasing effective stress conditions results in dilation of the sediment fabric and strain softening of the material. Strain softening promotes strain localization in narrow weak shear zones; and (c) deformation at a constant effective stress results in the sediment maintaining a constant shear strength and porosity (at average confining stresses below that resulting in the onset of cataclasis) with consequently little change in shear zone thickness once a stable configuration is achieved.

In the Duck Creek Diapir contact relationships that were present during the early period of intrusion (Stage I) are now overprinted and obscured. However, from the general poor alignment of blocks preserved in the diapir center it appears the diapir may have intruded in a turbulent manner, suggesting it had a low viscosity and high water content. High water contents are only preserved in sediments at great depths if the effective stresses are very low (high fluid pressures).

During the latter period of intrusion (Stage II) less turbulent deformation occurred across very broad shear zones. Such broad deformation zones are most likely to develop under increasing effective stress conditions when progressive consolidation and strain hardening of the muddy matrix will lead to the widening of the marginal shear zones (Moore & Byrne 1987) at the expense of the weaker material in the core of the diapir. An increase in effective stress would also be consistent with a change in deformation mechanism from IPF to cataclastic deformation in the enclosed sandstone blocks (Stage II, Figs. 11 and 12). Initially, under increasing effective stresses (but below 1–5 MPa average effective confining stress, see Fig. 11) we expect that the deformation and pore volume reduction was accommodated by IPF in the sandstones; however, eventually the reduced porosity and increased effective stresses (Handin *et al.* 1963, Bishop 1966, Borradaile 1981, Knipe 1986) led to grain breakage and cataclasis.

During the latest period of intrusion (Stage III) the marginal zone became very narrow. The mud comprising it is currently less indurated and weaker than the internal regions of the diapir. We suggest that only progressive failure and deformation under decreasing effective stress conditions would have produced the necessary dilation and strain softening. This would also be consistent with the proposed change of deformation fabrics in the enclosed sandstone blocks from cataclastic back to IPF as the average effective stresses fell below approximately 1–5 MPa, and the porosity in the actively deforming zone increased (Stage III, Figs. 11 and 12).

One important complication that we have not taken into account is the fluctuation in fluid pressure suggested by the vein evolution and inclusion trails. Fluctuations in fluid pressure indicate that variations in effective stress would be superimposed on the general trends described above. We observed that the calcite veins in the transitional zone generally formed as extensional veins in boudins with their planes orientated sub-perpendicular to the proposed transport direction (Orange 1990) and we suggest that in the diapiric environment they formed as extensional shear veins (Secor 1965, 1969, Etheridge 1983). The increasing abundance of laumontite deposition along the actual shear fractures sub-parallel to the transport direction in the matrix towards the end of the diapiric history suggests that, when effective stress dropped and IPF again took over, true hydrofractures as well as extensional shears developed.

A further insight to come out of this study concerns the observation that despite the relatively low intrinsic permeability that would be expected in a body comprising muds, fracture controlled fluid flow allowed mineralizing fluids to increasingly influence digenesis in the diapir. Also note that the Hoh accreted sequences beneath the unconformity are largely mineralized by laumontite, clay and carbonate (Stewart 1974) but the Quinault slope cover sequences above the unconformity and around the diapir are not. This suggests that the mineralization affecting the buried accretionary wedge has risen up with and/or into the diapir preferentially, with the possibility that relatively high temperature fluids of a 'Hoh-type' chemistry at least episodically fluxed though the confined conduit formed by the intrusion. This advection of fluids up through the diapir may have been confined to periods when the pore pressures episodically increased to allow the dilation of extensional shear or hydrofractures in the muddy matrix of the mélange.

The nature of mud diapirs intruding along other potential stress trajectories

We have discussed the reasons why the general stress trajectory, depicted as Path A in Figs. 11 and 14, can be inferred from the geometry and microfabric evolution in the Duck Creek diapir. Other stress trajectories are also possible given different environmental conditions and we predict that, because of this, other diapirs could have different internal structures and morphologies. As many different stress trajectories are possible we will illustrate the consequences for diapiric development along only a few main paths (Fig. 14). In path B (Fig. 14) the diapir intrudes to the surface under decreasing effective stress conditions. If diapirism begins in the IPF field we would predict IPF fabric to predominate throughout the life of the diapir. In addition, we would expect either turbulent intrusion or only narrow, strain-softened, marginal shear zones accompanied by plug flow and little internal deformation other than the initial mobilization of the mass in the source region. In contrast, if a diapir moves from the CF field into the IPF field (Path C, Fig. 14) we would expect cataclastic fabrics to be preserved in the core and that IPF fabrics would significantly overprint the CF fabrics only in the strain softened marginal shear zones.

At this point we must point out that scaly fabrics and cataclastic fabrics have rarely, if ever, been reported from surface mud volcanoes and we suspect that many of the surface manifestations of diapirism have intruded

along paths confined to the low effective stress IPF field (Path B, Fig. 14). Brown (1990) pointed out that the abundance of methane (Hedburg 1974, Hovland & Judd 1988, Brown 1990) in many mud diapirs will greatly assist in propelling diapirs along this path because of the reduction in viscosity and density associated with methane ebullition (ex-solution) and subsequent expansion of microbubbles during unloading. Brown (1990) also suggested that in some instances very rapid advection of gas charged fluids may result in fluidization of the sediments (occurring in sediments that follow general paths like B_2, Fig. 14) and local diatreme activity above rising diapiric masses.

Diapirs that intrude under increasing effective stress conditions (Paths D and E, Fig. 14) will become progressively compacted and should be dominated by cataclastic fabrics that affect broad strain hardened marginal shear zones. Eventually the material may compact and become so dense and strong that all movement of the diapir ceases. Ancient diapirs now exposed as strongly foliated mélanges in deeply eroded accretionary wedges may have intruded along these paths. In some cases, upward intrusion may be at a rate slower than the tectonic or sedimentary thickening of the overburden. These diapirs should eventually compact and cease activity (Path E). It is, however, possible for some diapirs to be buried and still intrude along a constant or decreasing effective stress path (Path F, Fig. 14). These diapirs will continue to be active and perhaps even deform by IPF as long as they maintain their high degree of internal overpressuring. Low permeabilities, high burial rates, hydrocarbon generation and smectite dehydration will all greatly facilitate intrusion along this latter type of burial stress path.

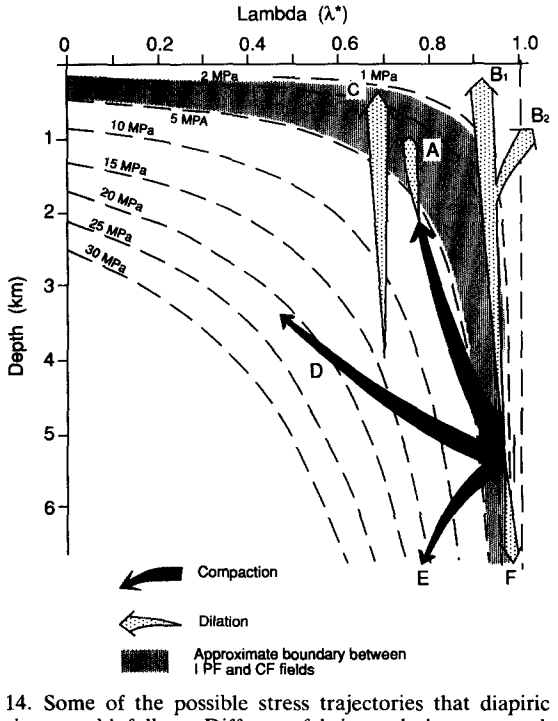

Fig. 14. Some of the possible stress trajectories that diapiric mud intrusions could follow. Different fabric evolutionary trends and distributions will be associated with each type of stress path. Again note that the compactive and dilative trends refer to the behavior of the muddy matrix while the IPF–cataclastic boundary (stipple) refers to fabrics that would develop in deformed sandstone blocks enclosed in the matrix.

SUMMARY

The Duck Creek mélange is exposed in the N–S-oriented sea cliffs of the Washington Coast. The Duck Creek mélange originated as a mud diapir in the accreted Hoh sequence of the Miocene–Pliocene Cascadia accretionary complex and intruded the overlying Quinault slope cover sequences in the mid to late Pliocene. At its current exposure level, the Duck Creek mélange is a lenticular shaped inclined dyke of sill-like intrusion. The diapir appears to have intruded laterally eastwards along a pre-existing normal fault that cuts the Quinault Formation, presumably originating from a major conduit seaward of the current cliff exposures. During its intrusion effective stress changes resulted in the spatial zonation and evolution of internal fabrics. Putting all the various observations on the general geometry, fabric evolution (spatial and temporal) and kinematic indicators together we have subdivided the intrusion history of the Duck Creek mélange into three main phases which form a part of an evolutionary spectrum of behavior.

Stage I

Early intrusion was accommodated by independent particulate flow (IPF) in much of the volume of the diapir. These early IPF fabrics are now best preserved in the diapiric core and suggest that effective stresses were initially very low. The primary disruption of any bedded structure in the original sedimentary source occurred during this period. The lack of obvious systematic block alignment associated with the regions in which this phase is best preserved is suggestive of a fairly turbulent intrusive pattern. It is possible that this turbulence dates from the period where the mud was intruding upwards in the large main feeder conduit (i.e. pre-sill formation).

Stage II

The intermediate period of intrusion was accommodated by cataclastic deformation across broad regions of the margins suggesting increased effective stresses during this period. The intensity of deformation rapidly decreases towards the core with the development of a plug-flow type intrusion. The broad marginal shear zones in which cataclastic fabrics are developed are consistent with the strain hardening that should have accompanied deformation under increasing effective stresses. Good correlation between clast long axes orientations, poles to extensional veins, and the current foliation patterns in the mélange suggest that this phase was not turbulent and was a prominent feature of the early lateral emplacement of the diapiric mélange as the sill-like body we see today. In addition, there appears to

have been some divergence in intrusion directions across the diapir suggesting it was spreading laterally. The diapir became increasingly important as a conduit to mineralizing fluids during this period with repeated syn-deformational calcite, plus minor quartz and zeolite veining associated with episodic fracture flow.

Stage III

This phase of intrusion was accommodated by independent particulate flow with intense scaly fabric development in a very limited region close to the wall rock–diapir contact. At this last stage the diapir was essentially intruding laterally as a stiff plug of material under falling effective stress conditions with strain softening of the consequently narrow marginal shear zone. Apart from dilatant fracture development and abundant zeolite deposition, little significant deformation occurred in the internal regions of the diapir at this stage. Zeolite deposition appears to have continued after the diapiric material was emplaced with dilatant scaly fractures becoming prime fluid conduits.

Acknowledgements—We thank Weldon Rau and an anonymous reviewer for constructive criticisms of this paper. We greatly appreciate the assistance of Gene Gonzales and John Krupp in the preparation of samples. In addition, we thank Casey Moore for his continued support, Weldon Rau for introducing us to the Duck Creek mélange, and Michael Allwright for his help with manuscript preparation. This research was supported by National Science Foundation Grants OCE 89U12272, EAR-8810789 and EAR-90053376. Acknowledgement is also made to the Donors of the Petroleum Research Fund, administered by the American Chemical Society, for the support of this research (ACS-PRF 23472-AC2 to J. C. Moore).

REFERENCES

Atkinson, J. H. & Bransby, P. L. 1978. *The Mechanics of Soils: An Introduction to Critical State Soil Mechanics*. McGraw-Hill, London.

Barber, A. J., Tjokrosapoeto, S. & Charlton, T. R. 1986. Mud volcanoes, shale diapirs, wrench faults and melanges in accretionary complexes, Eastern Indonesia. *Bull. Am. Ass. Petrol. Geol.* **70**, 1729–1741.

Behrmann, J. H. 1991. Conditions of hydrofracture and the fluid permeability of accretionary wedges. *Earth Planet. Sci. Lett.* **107**, 550–558.

Bishop, A. W. 1966. The strength of soils as engineering materials. *Geotechnique* **16**, 91–130.

Bishop, R. S. 1978. Mechanism for emplacement of piercement diapirs. *Bull. Am. Ass. Petrol. Geol.* **62**, 1561–1583.

Borradaile, G. J. 1981. Particulate flow of rock and the formation of cleavage. *Tectonophysics* **72**, 305–321.

Breen, N. A., Silver, E. A. & Hussong, D. H. 1986. Structural styles of an accretionary wedge south of the island of Sumba, Indonesia, revealed by seaMARC II side scan sonar. *Bull. geol. Soc. Am.* **97**, 1250–1261.

Brown, K. M. 1987. Physical and structural processes in accretionary complexes: the role of fluids in convergent margin development. Unpublished Ph.D. thesis, Durham University.

Brown, K. M. 1990. The nature and hydrogeologic significance of mud diapirs and diatremes for accretionary systems. *J. geophys. Res.* **95**, 8969–8982.

Brown, K. M. & Westbrook, G. K. 1988. Mud diapirism and subcretion in the Barbados Ridge Complex. *Tectonics* **7**, 613–640.

Byrne, T. 1984. Structural geology of melange terranes in the Ghost Rocks Formation, Kodiak Islands, Alaska. In: *Melanges, Their Nature and Origin and Significance* (edited by Raymond, L. A.). *Spec. Pap. geol. Soc. Am.* **198**, 21–52.

Etheridge, M. A. 1983. Differential stress magnitudes during regional deformation and metamorphism: Upper bound imposed by tensile fracturing. *Geology* **11**, 231–234.

Freeman, B. 1985. The motion of rigid ellipsoidal particles in three-dimensional slow flows: Implications for geological strain analysis. *Tectonophysics* **132**, 297–309.

Gilreath, J. A. 1968. Electric-log characteristics of diapiric shale. Diapirism and diapirs. *Mem. Am. Ass. Petrol. Geol.* **8**, 137–144.

Ghosh, S. K. & Ramberg, H. 1976. Reorientation of inclusions by a combination of pure shear and simple shear. *Tectonophysics* **34**, 1–70.

Handin, J., Hager, R. V. Friedman, M. & Feather, J. M. 1963. Experimental deformation of sedimentary rocks under confining pressure: Pore pressure tests. *Bull. Am. Ass. Petrol. Geol.* **47**, 717–755.

Hedberg, H. D. 1974. Relation of methane generation to undercompacted shales, shale diapirs and mud volcanoes. *Bull. Am. Ass. Petrol. Geol.* **58**, 661–673.

Henry, P., Le Pichon, X., Lallemant, S., Foucher, J. P., Westbrook, G. K. & Hobart, M. 1990. Mud volcano field seaward of the Barbados Accretionary Complex: A deep-towed side scan sonar survey. *J. geophys. Res.* **95**, 8917–8930.

Higgins, G. E. & Saunders, J. B. 1967. Report on 1964 Chatham mud island Erin Bay, West Indies. *Bull. Am. Ass. Petrol. Geol.* **51**, 183–189.

Higgins, G. E. & Saunders, J. B. 1974. Mud volcanoes—their nature and origin: Contribution to the Geology and Paleobiology of the Caribbean and Adjacent Areas. *Verh. naturf. Ges. Basel* **84**, 101–152.

Hovland, M. & Curzi, P. V. 1989. Gas seepage and assumed mud diapirism in the Italian central Adriatic Sea. *Mar. & Petrol. Geol.* **6**, 161–276.

Hovland, M. & Judd, A. G. 1988. *Seabed Pockmarks and Seepages: Impact on Geology, Biology and the Marine Environment*. Graham and Trotman, London.

Jones, M. E. & Addis, M. A. 1986. The application of stress path and critical state analysis to sediment deformation. *J. Struct. Geol.* **8**, 575–580.

Karig, D. E. 1986. Physical properties and mechanical state of accreted sediments in the Nankai Trough, Southwest Japan Arc. In: *Structural Fabrics in Deep Sea Drilling Project Cores From Forearcs* (edited by Moore, J. C.). *Mem. geol. Soc. Am.* **166**, 117–134.

Knipe, R. J. 1986. Deformation mechanism path diagrams for sediments undergoing lithification. In: *Structural Fabrics in Deep Sea Drilling Project Cores From Forearcs* (edited by Moore, J. C.). *Mem. geol. Soc. Am.* **166**.

Kugler, H. G. 1939. Visit to Russian oil districts. *J. Inst. Petrol.* **25**, 68–88.

Larue, D. K. & Hudleston, P. J. 1987. Foliated breccias in the active Portugese Bend complex, California: Bearing on melange genesis. *J. Geol.* **95**, 407–422.

Le Pichon, X., Foucher, J. P., Boulegue, J., Henry, P., Lallement, S., Benedetti, M., Avedik, F. & Mariotti, A. 1990. Mud volcano field seaward of the Barbados Accretionary Complex: a submersible survey. *J. geophys. Res.* **95**, 8931–8944.

Logan, J. M. & Rauenzahn, K. A. 1987. Frictional resistance of gouge mixtures of quartz and montmorillonite on velocity, composition and fabric. *Tectonophysics* **144**, 87–108.

Lucas, S. E. & Moore, J. C. 1986. Cataclastic deformation in accretionary wedges: Deep Sea Drilling Project Leg 66, southern Mexico, and on-land examples from Barbados and Kodiak Islands. In *Structural Fabrics in Deep Sea Drilling Project Cores From Forearcs* (edited by Moore, J. C.). *Mem. geol. Soc. Am.* **166**, 89–103.

Maltman, A. 1984. On the term 'soft sediment deformation'. *J. Struct. Geol.* **6**, 589–592.

McClellan, P. H. & Snavely, P. D., Jr. 1987. Multichannel seismic reflection profiles collected in 1977 off of the Washington–Oregon coast. *U.S. geol. Surv. Open-file Rep.* **87-607**.

Moore, J. C. & Byrne, T. 1987. Thickening of fault zones: a mechanism of melange formation in accreting sediment. *Geology* **15**, 1040–1043.

Morrow, C. A. & Byerlee, J. D. 1989. Experimental studies of compaction and dilatancy during frictional sliding on faults containing gouge. *J. Struct. Geol.* **7**, 815–825.

Musgrave, A. W. & Hicks, W. G. 1968. Outlining shale masses by geophysical methods. Diapirism and diapirs. *Mem. Am. Ass. Petrol. Geol.* **8**, 122–136.

Orange, D. 1990. Criteria helpful in recognizing shear-zone and diapiric melanges: Examples from the Hoh accretionary complex, Olympic Peninsula, Washington. *Bull. geol. Soc. Am.* **102**, 935–951.

Pickering, K. T., Agar, S. M. & Ogawa, Y. 1988. Genesis and

deformation of mud injections containing chaotic basalt–limestone–chert associations: Examples from the southwest Japan forearc. *Geology* **16**, 881–885.

Price, L. C. 1983. Geologic time as a parameter in organic metamorphism and vitrinite reflectance as an absolute paleogeothermometer. *J. Petrol. Geol.* **6**, 5–38.

Rau, W. W. 1970. Foraminifera, stratigraphy, and paleoecology of the Quinault Formation, Point Grenville–Raft River coastal area, Washington. *Bull. Wash. State Dept. Nat. Resourc.* **62**.

Rau, W. W. 1973. Geology of the Washington coast between Point Grenville and the Hoh River. *Bull. Wash. State Dept. Nat. Resourc. Geol. & Earth Resourc. Div.* **66**.

Rau, W. W. 1975. Geologic map of the Taholah and Destruction Island quadrangles, Washington, scale 1:62,500. Washington State Department of Natural Resources.

Rau. W. W. 1979. Geologic map in the vicinity of the Lower Bogachiel and Hoh Rivers, and the Washington coast, geologic map GM-24. Washington State Department of Natural Resources.

Rau. W. W. 1987. Mélange rocks of Washington's Olympic coast. *Geol. Soc. Am. Centennial Field Guide, Cordilleran Sect.*, 373–376.

Rau, W. W. & Grocock, G. R. 1974. Piercement structure outcrops along the Washington coast. *Wash. Div. Mines & Geol. Inform. Circ.* **51**.

Rau, W. W. & McFarland, C. R. 1982. Coastal wells of Washington. *Wash. Div. Geol. & Earth Resourc. Rep. Invest.* **26**.

Reed, D. L., Silver, J. E., Tagudin, J. E., Shipley, T. H. & Vrolijk, P. 1990. Relationships between mud volcanoes, thrust deformation, slope sedimentation and gas hydrate, offshore north Panama. *Mar. & Petrol. Geol.* **7**, 44–54.

Ridd, M. F. 1970. Mud volcanoes in New Zealand. *Bull. Am. Ass. Petrol. Geol.* **54**, 601–616.

Riddihough, R. P. 1977. A model for recent plate interactions off Canada's west coast. *Can J. Earth Sci.* **14**, 384–396.

Roscoe, K. H., Schofield, A. N. & Wroth, C. P. 1958. On the yielding of soils. *Geotechnique* **8**, 22–53.

Secor, D. T. 1965. Role of fluid pressure in jointing. *Am. J. Sci.* **263**, 633–646.

Secor, D. T. 1969. Mechanics of natural extension fracturing at depth in the earth's crust. *Geol. Surv. Pap. Can.* **68-52**, 3–48.

Schofield, A. N. & Wroth, C. P. 1968. *Critical State Soil Mechanics*. McGraw-Hill, London.

Shi, Y. & Wang, C. Y. 1988. Generation of high pore pressures in accretionary prisms—inferences from the Barbados subduction complex. *J. geophys. Res.* **93**, 8893–8910.

Snavely, P. D., Jr. & Kvenvolden, K. A. 1988. Preliminary evaluation of the petroleum potential of the Tertiary accretionary terrane, west side of the Olympic Peninsula, Washington: Part A—Geology and hydrocarbon potential. *Bull. U.S. geol. Surv.* **1892**, 1–17.

Snavely, P. D., Jr. & Wagner, H. C. 1982. Geologic cross-section across the continental margin of southwestern Washington. *U.S. geol. Surv. Open-file Rep.* **82-459**.

Stewart, R. 1970. Geologic map of the Hoh River-Queets River area, Olympic Peninsula, Washington. Unpublished M.A. thesis, University of Washington, Seattle.

Stewart, R. 1974. Zeolite metamorphism of sandstone in the western Olympic Peninsula, Washington. *Bull. geol. Soc. Am.* **85**, 1139–1142.

Tabor, R. W. & Cady, W. M. 1978. Geologic map of the Olympic Peninsula, Washington. Map I-994. *U.S. geol. Surv. Misc. Invest. Ser.*

Westbrook, G. K. & Smith, M. J. 1983. Long decollements and mud volcanoes: Evidence from the Barbados Ridge complex for the role of high pore-fluid pressure in the development of an accretionary complex. *Geology* **11**, 279–283.

Williams, P. R., Pigram, C. J. & Dow, D. B. 1984. Melange production and the importance of shale diapirism in accretionary terrains. *Nature* **309**, 145–146.

WNP-3. 1986. WNP-3 Geologic Support Services coastal terrace study. Golder Associates, Washington Public Power Supply System, 3000 George Washington Way, Richland, Washington.

Zhang, J., Wong, T. F. & Davis, D. M. 1990. Micromechanics of pressure-induced grain crushing in porous rocks. *J. geophys. Res.* **95**, 341–352.

Zoback, M. D. & Byerlee, J. D. 1976. Effect of High pressure deformation on permeability of Ottawa Sand. *Bull. Am. Ass. Petrol. Geol.* **60**, 1531–1542.